Remote Sensing Applications: Society and Environment 40 (2025) 101774

Contents lists available at ScienceDirect

Remote Sensing Applications: Society and Environment

journal homepage: www.elsevier.com/locate/rsase

Aboveground dry biomass modeling with Remotely Piloted Aircraft in Brazilian Savanna: a case study in an experimental area under reduced-impact logging (2005–2021)

Paola Aires Lócio de Alencar [a,*], Alba Valéria Rezende [a], Marcus Vinicio Neves d'Oliveira [b], Eder Pereira Miguel [a], Hallefy Junio de Souza [a], Roberta Franco Pereira de Queiroz [a]

[a] College of Technology, Department of Forest Engineering, University of Brasília, Campus Darcy Ribeiro, Asa Norte, Brasília, DF, 70910-900, Brazil
[b] Brazilian Agricultural Research Corporation, Embrapa Acre, Rodovia BR-364, Km 14, Rio Branco, Acre, 69900-970, Brazil

ARTICLE INFO

Keywords:
Carbon mapping
Cerrado biome
Photogrammetry
Forest monitoring
Post-logging recovery

ABSTRACT

Savanna ecosystems are critical for carbon storage and biodiversity conservation, yet their structural complexity challenges biomass estimation. This study evaluates the applicability of using RGB imagery acquired by a Remotely Piloted Aircraft (RPA), through the Structure for Motion (SfM) approach, to build a statistical model for estimating aboveground dry biomass (AGB) in a cerrado *sensu stricto* area of the Brazilian Cerrado biome. The research was conducted from 2005 to 2021 in a 2.1 ha experimental area located at Fazenda Água Limpa (FAL), a research and conservation area of the University of Brasília, Federal District, Brazil. A Canopy Height Model (CHM) was generated by subtracting the Digital Surface Model (DSM) from the Digital Terrain Model (DTM). Height metrics were derived from the CHM, and an Ordinary Least Squares regression model was fitted using data from 21 field plots (20 m × 50 m). The resulting model (AGB = −2.73 - 0.54·Elev_MAD_MODE + 2.56·Elev_P99 + ε) achieved $R^2 = 0.65$ and RMSE = 0.41 Mg 0.1 ha^{-1} (RMSE% = 18), and was used to map AGB across the sampled plots (2.1 ha) and the entire imaged area (10.4 ha). The estimated mean AGB was 25 ± 6.4 Mg ha^{-1}, consistent with forest inventory data. The total estimated AGB for the full imaged area was 24.6 Mg ha^{-1}. The model demonstrated potential for extrapolation to areas with similar structural characteristics.

1. Introduction

Human influence on the climate – evidenced by the warming of the atmosphere, oceans, and continents – is scientifically proven. According to the fifth Assessment Report of the Intergovernmental Panel on Climate Change (IPCC), since 1750, observed increases in greenhouse gas (GHG) concentrations in the atmosphere have been caused by human activities, and each of the last four decades has been successively warmer than any decade preceding it since 1850 (Shukla et al., 2019).

The brazilian Cerrado, the largest savanna in South America, covers more than 2 million km^2 (Lahsen et al., 2016) and stands out for its remarkable biodiversity and high degree of endemism (DANDOIS and ELLIS, 2010). Its physiognomies range from forested to savanna and grassland formations (Ribeiro; WALSTON et al., 2023).

* Corresponding author.
E-mail address: albavr@unb.br (P.A.L. de Alencar).

https://doi.org/10.1016/j.rsase.2025.101774
Received 12 August 2023; Received in revised form 13 October 2025; Accepted 22 October 2025
Available online 7 November 2025

Despite its ecological importance, the biome is under intense anthropogenic pressure. Nearly half of its original area has already been converted for agricultural and livestock purposes (SANKY et al., 2022; Beuchle et al., 2015). According to the 2023 Annual Deforestation Report, Brazil lost 561,861 ha of native vegetation in that year, with more than 60 % of this loss occurring in the Cerrado biome (MapBiomas, 2024).

Given its size and biological richness, the adoption of conservation strategies in the Cerrado is critical for maintaining ecosystem services (BRASIL. Ministério do Meio Ambiente, 2011). The biome is considered relevant to the global carbon balance (Poulter et al., 2014), although carbon stock and sequestration rates remain poorly understood across many of its vegetation types (Pugh et al., 2019; Duvert et al., 2020). Recent studies highlight its role as a carbon sink, particularly under varying disturbance and management regimes such as fire (Burkholder et al., 2021; Rügner et al., 2022).

Forest inventories have traditionally been used to estimate aboveground biomass and carbon stocks, based on field-based measurements with high technical rigor. However, logistical limitations, such as accessibility, seasonality, and financial constraints, often restrict their implementation over large or remote areas. In this context, remote sensing technologies have emerged as effective alternatives or complements, allowing for broader spatial coverage and more frequent monitoring (Houghton, 2012; González-Jaramillo, Fries and Bendix, 2019; Wulder et al., 2021).

Among the most promising tools are Remotely Piloted Aircraft (RPA), which combine low operational costs with the ability to produce high-resolution and on-demand spatial data tailored to specific study needs (Mlambo et al., 2017). Structure-from-Motion (SfM) photogrammetry based on RGB imagery has proven effective for three-dimensional vegetation modeling, especially in open-canopy environments like the Cerrado (Koh and Wich, 2012; Shin et al., 2018; Puliti et al., 2021).These techniques allow for the extraction of structural vegetation metrics—such as mean height, canopy variance, and density—that can be correlated with aboveground biomass (AGB) using allometric equations (Roitman et al., 2018; Mayr et al., 2023). The accuracy of this approach has been validated in various tropical and savanna ecosystems, demonstrating its applicability for biomass estimation at local and sub-regional scales (Walston et al., 2023; Silva et al., 2023; Díaz-Varela et al., 2023).

Specifically in the Cerrado, studies such as Araujo et al. (2024) have demonstrated the effectiveness of RGB data acquired by RPA for accurate AGB estimation in cerrado *sensu stricto* formations, reinforcing the potential of RPA platforms to support fast and high-resolution forest inventories. Other case studies conducted in similar physiognomies highlight the feasibility of this approach, even using low-cost sensors, and point to its applicability in national monitoring programs and carbon credit policies (Gülci et al., 2023; Bazzo et al., 2024).

Furthermore, the open-canopy structure of savanna ecosystems enhances the detection of subtle changes in canopy height and vegetation density using RPA, contributing both to carbon dynamics monitoring and the assessment of natural and anthropogenic disturbances (SANKY et al., 2022; Rügner et al., 2022).

In this study, the sampled area is located within a well-preserved site representative of cerrado *sensu stricto*, providing structural homogeneity that supports extrapolation of results. Although limited in extent, this approach has been validated by other small-scale studies that yielded consistent results aligned with regional patterns (Silva et al., 2023; Araujo et al., 2024).

RPA-based methods have become a practical and robust alternative for biomass estimation in tropical ecosystems, especially when high spatial accuracy is required over specific areas. This technology can also support carbon inventories, restoration planning, and carbon credit initiatives in diverse and threatened biomes such as the Cerrado (Gülci et al., 2023; Bazzo et al., 2024).

This study evaluated the applicability of RGB imagery acquired from of Remotely Piloted Aircraft (RPA) platforms, using Structure-from-Motion (SfM) photogrammetry, approach, to construct a mathematical model - for estimating aboveground dry biomass (AGB) in

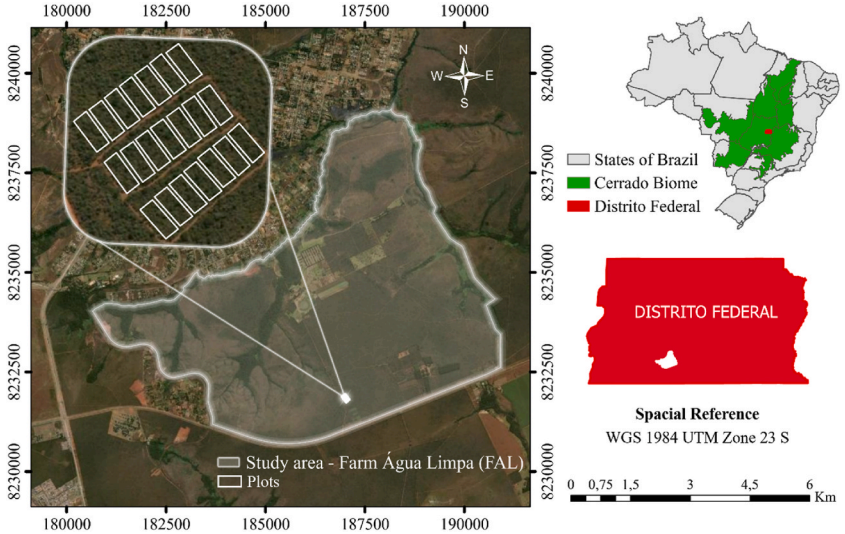

Fig. 1. Map of the location of the experimental area containing the 21 study plots at Farm Água Limpa (FAL), Federal District, Brazil.

a cerrado *sensu stricto* area. To achieve this, the following steps were carried out: (i) selection of the most relevant structural metrics extracted from the RPA-derived point cloud for AGB modeling; (ii) estimate of AGB and C stocks at the plot level; (iii) validation of the fitted model with using data from a nearby area with similar vegetation; and (iv) generation of an AGB map for the entire area surveyed by the RPA.

2. Methodology

2.1. Study area

The study was carried out in the experimental section of Fazenda Água Limpa (FAL), a research and conservation unit of the University of Brasília, located in Federal District, Brazil (Fig. 1). Situated at an average altitude of 1100 m, between the geographic coordinates 15°56′–15°59′ S and 47°53′–47°59′ W, FAL covers 4340 ha and is part of the Cerrado Biosphere Reserve.

According to the Köppen classification, the region's climate is of the Aw type, with average temperatures ranging from 12 to 28.5 °C (Alvares et al., 2013). The average annual precipitation is 1600 mm, with a well-defined dry season in the months of July to September. The soils are of the Latosols type, with high aluminum and low calcium and magnesium content (Abdala et al., 1998).

A large part of the total area of the FAL is covered by Cerrado physiognomic forms, with 2340 ha destined for preservation and 800 ha destined for conservation. The phytophysiognomies are represented by grassland, savanna and gallery forest, formations, but the cerrado *sensu stricto*, that is a savanna phytophysiognomie, predominates at the site, occupying about 1480 ha.

2.2. Forest inventory

For this study, we selected an area of cerrado *sensu stricto* where silvicultural treatments were applied. In 2005, was implemented an experiment seeking to simulate, monitor and evaluate different strategies for timber exploitation of the cerrado *sensu stricto* to energy production.

The experiment consisted of 3 (three) blocks of 0.85 ha (50 m × 170 m) systematically distributed in the area. The site for the first block was chosen randomly, and the other blocks were demarcated parallel to the first, maintaining a minimum distance of 20 m between the blocks (Fig. 1). In 2005, the vegetation structure and floristics in the three blocks were very similar. The density, total height, and base diameter measured at 30 cm from ground level (Db) of all woody individuals with Db equal to or greater than 5 cm averaged 1427 ind ha^{-1}, 3 m, and 8.2 cm, respectively. At the time, the variability recorded for each of these variables was low (6 %). Floristic similarity measured by the Sørensen index (Margurran, 1988) among the three blocks high (0.9) species richness averaged 49 woody species per block.

Each block was divided into seven 20 m × 50 m (0.1 ha) plots, separated from each other by a 5 m × 50 m (250 m^2) firebreak, as shown in Fig. 1. The plots were permanently installed, and their vertices were demarcated with iron stakes to ensure exact plot boundaries over time. Each plot was further subdivided into 10 subplots of 10 m × 10 m, whose vertices were also demarcated with iron stakes.

Additionally, in 2005, after the establishment of the blocks and demarcation of the plots and subplots, we conducted a forest inventory in the three blocks, considering all woody vegetation, trees and shrubs, living and dead standing. As the tortuosity of the stem is a natural characteristic of most woody individuals of the cerrado *sensu stricto* (Gomes et al., 2007), the value of Db was obtained from the average of the diameters taken with a caliper in two directions perpendicular to the stem. The total height (Ht) of each stem was measured with a 12 m telescopic ruler. Higher heights were estimated. Individuals with more than one stem protruding below 30 cm from the ground, with Db ≥ 5 cm, had each stem measured separately. All trees were labeled with an aluminum plate containing an identification number. We botanically identified all individuals in family, genus and species levels and recorded their X and Y coordinates in meters.

In 2006, we implemented five silvicultural treatments simulating different intensities of timber exploitation in each block. Each treatment was implemented in a 0.1 ha permanent plot of each block. Two permanent plots of each block were kept as controls. The distribution of treatments and controls within each block was randomized. The treatments implemented in each block were T1 — thinning of 50 % of the basal area of woody individuals with Db ≥ 5 cm, regardless of species; T2 — thinning of 50 % of the basal area of woody individuals with Db ≥ 5 cm, regardless of species; T3 — thinning of 100 % of the basal area of woody individuals with Db ≥ 5 cm, belonging to species with energy potential (*Tachigali vulgaris, Dalbergia miscolobium* and *Pterodon pubescens*); T4 — thinning of 50 % of the basal area of woody individuals with Db ≥ 5 cm, belonging to species with energy potential (*Tachigali vulgaris, Dalbergia miscolobium* and *Pterodon pubescens*); T5 — thinning of 100 % of the basal area of woody individuals with Db ≥ 5 cm, belonging to *Tachigali vulgaris*; T6 and T7 — control or witness areas, without any silvicultural intervention.

In T1, we evaluated the response of the woody community over time after clear cutting of the woody vegetation, regardless of species, which is the type of exploitation commonly performed in areas of cerrado *sensu stricto*. In T2, we evaluated the behavior of the community by removing only 50 % of the basal area, regardless of species. As for the implementation of T3 and T4, we evaluated the community response when the exploration included only individuals belonging to species considered to have energy production potential (Tachigali vulgaris, Dalbergia miscolobium and Pterodon pubescens). The objective of T5 was to evaluate the community response over time when harvesting involves thinning only individuals of Tachigalli vulgaris (100 % of basal area), commonly known as the charcoal tree, which is the species with the greatest potential for energy production in this physiognomy.

In 2008, 2012, 2015, and 2021, i.e., 2, 6, 9, and 15 years after logging, we conducted remediation of the woody vegetation in all plots in each block. The variables Db and total height of the stems, with Db ≥ 5 cm, of all living and dead standing individuals recorded

in a previous measurement and that remained in the plots in the next measurement were measured. We also recorded individuals with Db $\geq$ 5 cm who died or were recruited during each monitored period (2006–2008, 2008 to 2012, 2012 to 2015, and 2015 to 2021). Recruited individuals had their X and Y coordinates recorded, were botanically identified, labeled with an aluminum plate containing an identification number, and their Db and total height variables were measured.

From 2012, the botanical classification system was updated to APG III (Angiosperm Phylogeny Group) (Bremer et al., 2009) and the botanical nomenclature was checked and updated with the help of the Reflora Virtual Herbarium (http://reflora.jbrj.gov.br), managed by the Research Institute of the Botanical Garden of Rio de Janeiro.

For this study, we only used data from the survey conducted in 2021, that is, 15 years after the exploration.

2.3. Estimation of dry aboveground biomass from the forest inventory data

From the 2021 inventory data, we estimated the aboveground dry woody biomass of each woody individual sampled in the 0.1 ha plots using an allometric equation adjusted for the local cerrado *sensu stricto* (Rezende et al., 2006), given by:

$$AGB = 0.4913 + 0.0291 * Db^2 * H \quad (R^2 = 98.28\% \text{ and RSME} = 25.79\%) \tag{1}$$

where AGB is the aboveground dry woody biomass of the stem, in Kg; Db is the diameter of the stem taken at 0.30 m from the ground (cm); H is the total height of the stem (m); R^2 is the coefficient of determination; and RSME is the relative root mean square error.

Next, we estimated the total AGB of each 0.1 ha plot. For the purpose of this study, the stocks of AGB estimated from field data (Db and H) will be referred to as observed AGB values.

Based on the data obtained by the 2021 forest inventory we also statistically compared the stocks of woody individual density and observed AGB that were recorded in the areas subjected to each of the 7 silvicultural treatments, in order to assess whether these stocks were statistically equal about 15 years after the logging interventions. Therefore, density and AGB data were submitted to analysis of variance considering a randomized block design (ZAR, 1999) and a 5 % significance level. The assumptions of normality and homogeneity of variances were considered in the analyses and the means of the treatments were compared by the Tukey test (ZAR, 1999).

2.4. Remotely piloted aircraft (RPA) data

The photogrammetric survey conducted in October 2020utilized a class III Remotely Piloted Aircraft (RPA), DJI brand, Phantom 4 Pro multirotor model, equipped with a GNSS system (GPS and Glonass) of high sensitivity, in addition to accelerometer, barometer, compass, gyroscope and an RGB camera model FC330 (20 MP, 4000 $\times$ 3000 pixels), with a 24 mm lens (equivalent to a 35 mm lens), mounted on a 3-axis electronic gimbal (Fig. 2). The maximum flight range, according to the RPA manufacturer, was 30 min (DJI Phantom 4 Pro/Pro+, 2017). The remote-control system integrates a dual-frequency (2.4 and 5.8 GHz) downlink video system, with a 7 km range (FCC), compatible with Android and iOS.

An RGB-only sensor approach was adopted based on three main criteria:

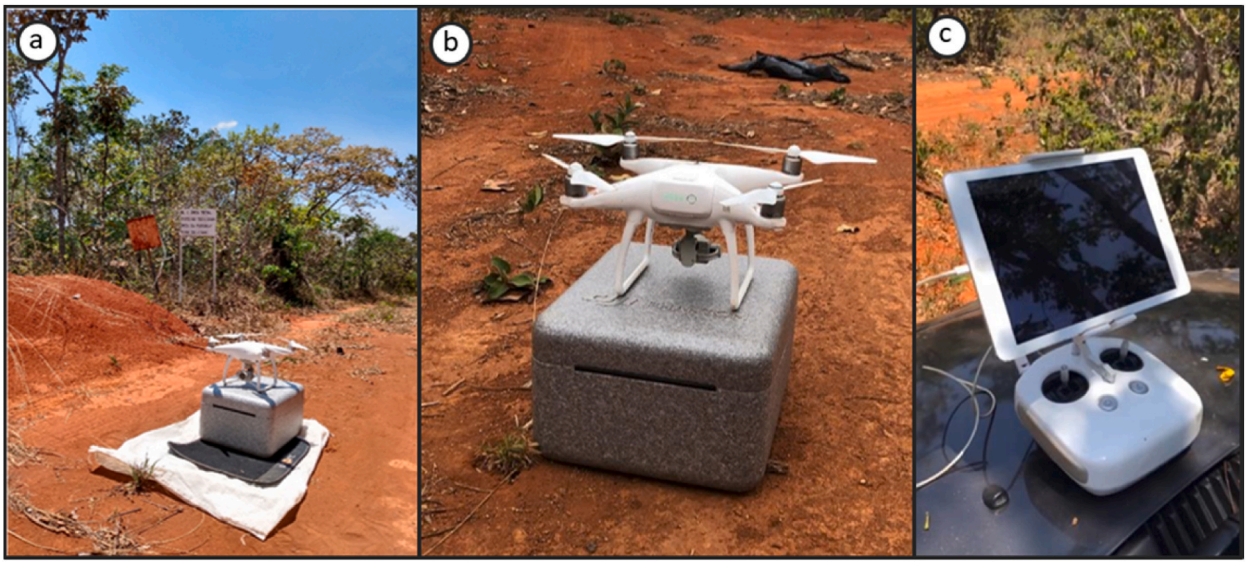

Fig. 2. a) Remotely Piloted Aircraft (RPA), DJI Phantom 4 Pro positioned to begin overflying the area b) RPA after overflying the area; and c) Remote Control and Apple iPad second generation A8 chip.

(1) Cerrado-specific suitability – The open-canopy structure (<50 % cover) of cerrado *sensu stricto* allows sufficient ground visibility through RGB spectra, as demonstrated in recent savanna studies (BERA et al., 2022; Queiroz et al., 2023);
(2) Cost-effectiveness – RGB sensors provide adequate data for aboveground biomass modeling at less than 20 % of the cost of multispectral or LiDAR systems (Cunliffe et al., 2021);
(3) Validation precedence – Successful AGB estimations using RGB-derived metrics (e.g., CHM) have already been validated for neotropical savannas (Almeida et al., 2023).

We performed the nadir flight autonomously, with a constant speed of 45 km h^{-1}, 85 % front and side overlap between the tracks, and 90 m above ground height. At this altitude, the ground sampling distance (GSD) of the images was 3.9 cm. The flight lasted 12 min and covered an area of 10.4 ha.

To ensure the accuracy and precision of the process, we accurately georeferenced the vertices of each plot and specific points on the roads surrounding the blocks with a DGPS Zenite II dual frequency receiver (L1 and L2), with collection time of 10–15 min (Fig. 3). In addition, five ground control points (GCPs) were well distributed in the area. The distribution patterns of the five GCPs sought to better contribute to georeferencing (Fig. 4).

After the overflight, we processed the 2D aerial images, overlaid and displaced using Pix4D Mapper software. We then applied the SfM technique to the set of 158 2D images produced, aiming to generate the 3D point clouds and the following products: (i) orthophoto mosaic, (ii) digital surface model (DSM), and (iii) digital terrain model (DTM).

We used the Scale-Invariant Feature Transform (SIFT) algorithm, whose correspondence requires key points and visually differentiated textures in the images (Lowe, 2004). SIFT allows image position, orientation, and geometry to be reconstructed simultaneously from automatically identifying matching features in the various images, even if there are large-scale variations (Nyimbili et al., 2016).

To construct the DTM, we followed the procedure employed by Mlambo et al. (2017) and WALSTON et al. (2023), which does not require external sources of elevation data for modeling, such as LiDAR data (D'OLIVEIRA et al., 2021) since the cerrado *sensu stricto* areas have a canopy cover of less than 50 %.

Therefore, we based the direct use of the DTM on the following characteristics of the study area: 1) relatively small size of the area; 2) flat terrain with exposed soil at several points (with roads bypassing the experimental blocks); and 3) sparse and not very dense vegetation. To validate the DTM produced by photogrammetry, we compared the elevation of the points collected by DGPS with those of the DTM produced by Pearson's correlation.

We then used the FUSION LiDAR package (USDA Forest Service) to process the data from the RPA (Mcgaughey, 2009). We cut out

Fig. 3. a) Ground control point (GCP) at the vertex of the permanent plot, made with cardboard and a white sheet. The white sheet aimed to ensure good reflectance for identification in the image captured by the DJI Phantom4 Pro; b) Geodetic DGPS collecting X, Y coordinates and Z elevation of the permanent plot vertices; c) visualization of the target in the orthomosaic.

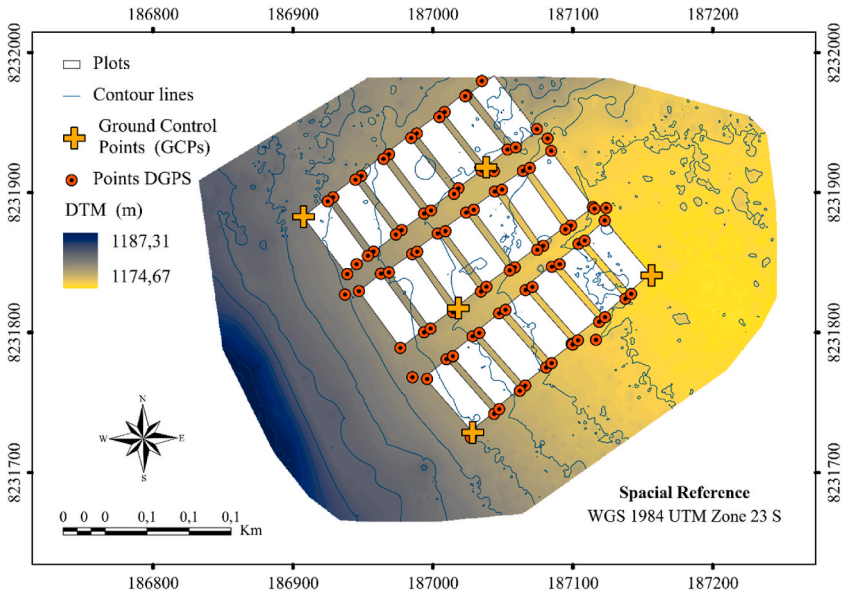

Fig. 4. Location of the five ground control points (GCPs) and 86 DGPS points collected at the vertices of the field plots and at specific points on the roads.

the 3D point cloud for the areas referring to the plots (*Polyclipdata*). To do this, polygons were produced in ArcGIS PRO from the coordinates of the vertices of each plot georeferenced in the field. Next, we performed the normalization of the point cloud (*Subtractground*), to obtain the height of the targets (z-axis) disregarding the elevation.

From the DSM and DTM, both produced at 1 m spatial resolution, we derived the canopy height model (CHM = DSM - DTM). Table 1 lists the metrics extracted from the point cloud (*Cloudmetrics*).

Fig. 5 illustrates the overall data acquisition and processing workflow.

2.5. Estimation of dry aboveground biomass using data obtained by RPA

To model AGB (response variable) as a function of height metrics extracted from the normalized point cloud (predictor variables), we considered the observed AGB of each of the 21 permanent plots sampled in the field, as well as the respective values of their metrics. Initially, all data were subjected to the Shapiro-Wilk normality test (Shapiro; Wilk, 1965).

Next, we calculated the Pearson correlation between all variables involved in the model to assess the existence of multicollinearity among the predictor variables and the existence of a high correlation between the predictor variables and the response variable.

Metrics (predictive variables) multicollinear, with significant correlation (r) (p-value <0.05) and greater than 0.7 were excluded from the model, and metrics whose correlation with the response variable (observed AGB) was significant (p-value <0.05) and greater than 0.7 were selected. Data analysis was performed using R software (R Core Team, 2015).

To model AGB (response variable) as a function of height metrics extracted from the normalized point cloud (predictor variables),

Table 1
Height metrics extracted from the normalized point cloud generated for each plot sampled in the field.

Metrics	Description (Code)
1	Maximum (Elev.maximum)
2	Average (Elev.mean)
3	Mode (Elev.mode)
4	Mode of general absolute deviations (Elev.MAD.mode)
5	Standard deviation (Elev.stddev)
6	Variance (Elev.variance)
7	Coefficient of variation (Elev.CV)
8	Interquartile distance (Elev.IQ)
9	Asymmetry/obliquity (Elev.skewness)
10	Elev L1, L2, L3 e L4
11	Kurtosis (Elev.Kurtosis)
12	Mean Square Elevation (Elev.SQRT.mean.SQ)
13	Average Cubic Elevation (Elev.CURT.mean.CUBE)
14	Canopy Relief Ratio (canopy.relief.ratio)
15	Percentiles 5°, 10°, 20°, 25°, 30°, 40°, 50°, 60°, 70°, 75°, 80°, 90°, 95°, 99° (Elev.Px)

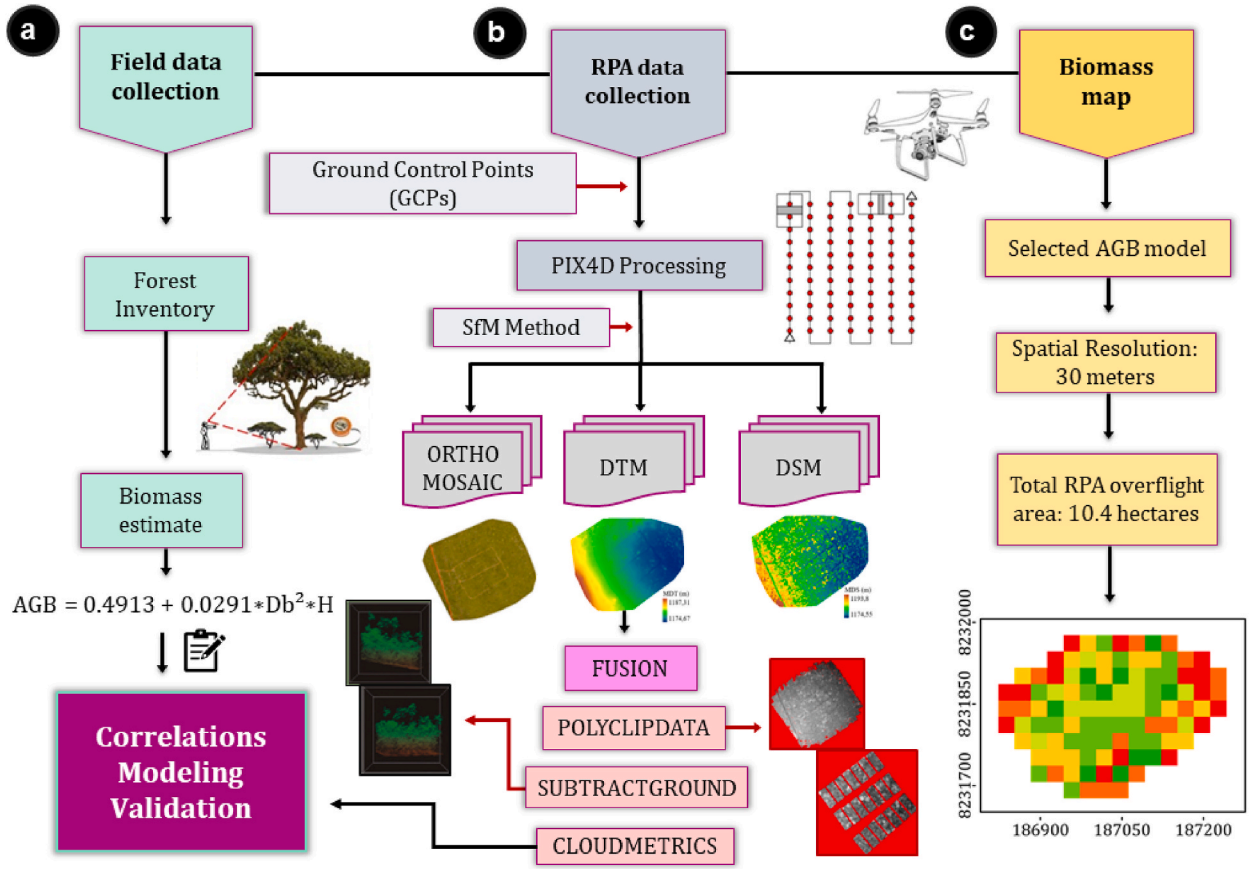

Fig. 5. Workflow for collecting and processing RGB data from the RPA. Field data collection (left), AGB modeling (center), and AGB map generated from the selected equation (right).

we initially considered AGB stocks obtained from 21 permanent field plots, along with their respective metric values. To improve model accuracy and robustness, we expanded the dataset by including an additional 18 plots (0.1 ha each) of cerrado *sensu stricto*, located approximately 2.5 km away from the main experimental area,

These additional plots were carefully selected to ensure similarity in abiotic conditions (such as altitude, topography, and soil characteristics) and in woody vegetation structure and floristic composition to the original plots. This selection minimizes spatial heterogeneity and potential biases, enhancing the model's representativeness and extrapolation power for cerrado *sensu stricto* areas with similar environmental conditions. The same procedures used to obtain AGB stocks and height metrics for the original plots were applied to the additional ones, maintaining data consistency.

Before modeling, all data from the 39 plots were submitted to the Shapiro-Wilk normality test (Shapiro; Wilk, 1965). Next, we calculated Pearson's correlation between all variables involved in the modeling, in order to assess the existence of multicollinearity among predictor variables and high correlation between predictor variables and the response variable. Multicollinear metrics (predictor variables) with significant correlation (r) (p-value <0.05) and higher than 0.7 were excluded from the modeling. On the other hand, metrics whose correlation with the response variable (observed AGB) was significant (p-value <0.05) and greater than 0.7 were selected. Data analysis was performed by R software (R Core Team, 2015).

Another criterion used in the selection of the predictor variables was the variance inflation factor (VIF), which is a second measure of the presence of multicollinearity among the predictor variables. The higher the VIF, the more severe the multicollinearity (Neter et al., 1996). Therefore, predictor variables with VIF greater than 5 were also excluded from modeling. The VIF value is given by:

$$VIF_j = \frac{1}{\left(1 - R_j^2\right)} \quad j = 1, 2, 3, \ldots, p \tag{2}$$

where R_i^2 is the multiple correlation coefficient resulting from the regression of Xj on the other p−1 predictor variables and p is the number of predictor variables.

Once the predictor variables were defined, we used the "Stepwise" procedure of selecting significant variables (Drapper; SMITH et al., 2023) to generate the AGB model, which can be expressed by:

$$Y = \beta_0 + \beta_1 . X_1 + \beta_2 . X_2 + \ldots + \beta_i . X_i + \varepsilon \quad (3)$$

where Y is the value of the response variable; $\beta_0, \beta_1, \beta_2, \ldots, \beta_i$ are parameters of the model, where β_0 is a constant (intercept) and β_1, β_2 …. e β_i are the angular coefficients; X_1, X_2, ….. e X_i are the height metrics derived from point clods generated by SfM, and ε is the error associated with the model.

To evaluate the accuracy of the adjusted AGB model we considered the following accuracy statistics: adjusted coefficient of determination (R^2aj), absolute root means square error (RMSE); relative root mean square error (RMSE%) and graphical distribution of residuals (Draper; SMITH et al., 2023). In addition, we also used Akaike's Information Criterion (AIC), which is a measure of quality of fit that aims to improve the selection of regression models (Akaike, 1973) and is given by:

$$AIC = -2 \log(\widehat{\theta}) + 2(k) \quad (4)$$

where $\widehat{\theta}$ is the maximum value of the likelihood function, and k is the number of parameters to be estimated in the model.

The smaller the AIC value, the better the evaluation received by the model (Akaike, 1973). Thus, the entry of a variable into the model occurs if the AIC value related to that variable is lower than the other variables. In addition, the AIC value of the overall model decreased with each variable.

All analyses of AGB model fit by the "Stepwise" procedure were done from the lm (de linear model) function of the basic statistical analysis packages of R software (R Core Team, 2015).

To validate the adjusted AGB model we used the leave-one-out cross-validation (LOOCV) method, employing the functions "trainControl" and "train" from the caret package, available in R software (Kuhn, 2008). The LOOCV cross-validation allows to evaluate the generalization ability of a regression model when one does not have enough data that can be used in the application of statistical tests for model validation (Peduzzi et al., 2012). This validation method consists of performing several interactions and at each interaction creating a model with n-1 data, considering n the total number of data, which in the present study was 39. Each model fitted with n-1 data is validated with the data not included in the fit. Therefore, we performed 39 interactions and for each interaction we calculated the RMSE (root mean square error absolute) and R^2 (coefficient of determination) metrics. The validation result was obtained from the averages of the 39 values for each accuracy metric evaluated.

Once the adjusted model was validated, we statistically compared the estimated AGB values of the plots submitted to the 7 silvicultural treatments, with the AGB values, considering a randomized block design (ZAR, 1999), at 5 % significance level. The assumptions of normality and homogeneity of variances were considered in the analysis and the means of the treatments were compared by the Tukey test (ZAR, 1999).

2.6. *Spatialization of the AGB*

Following the methodology detailed by d'Oliveira et al. (2014), we created 30 m × 30 m raster layers from the point cloud for the selected height metrics (*Elev_MAD_MODE* and *Elev_P99*). This resolution was chosen because:

(1) It provides optimal correspondence with our field plot dimensions (1000 m^2 vs. 900 m^2 pixel area), ensuring direct validation;
(2) It matches the operational scale of cerrado *sensu stricto* vegetation structure;
(3) It enables compatibility with medium-resolution satellite monitoring systems;

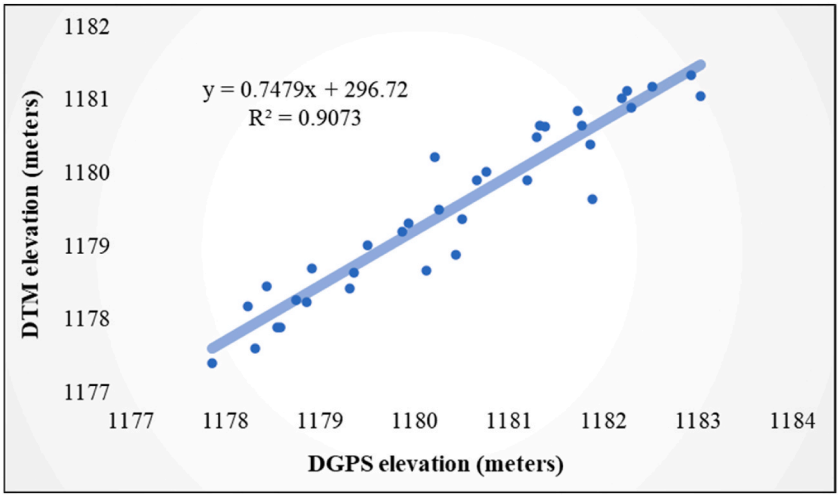

Fig. 6. Correlation plot of the DTM elevation values produced by Pix4D using the SfM method with the elevation values obtained directly by DGPS in the field.

(4) It effectively balances detail and computational efficiency from the original 3.9 cm GSD data.

The validated AGB model (R^2 = 0.65, RMSE = 0.41 Mg 0.1 ha^{-1}) was then applied following d'Oliveira et al.'s (2014) spatial prediction framework to generate a wall-to-wall biomass map of the 10.4 ha study area.

3. Results

3.1. Digital terrain model

When evaluating the correlation of the elevation values contained in the DTM produced by Pix4D software, through the SfM technique, with the elevation values obtained in the field, with DGPS, at the vertices of the experimental plots and at strategic locations of the roads surrounding the experimental blocks (excluding the GCPs), we verified that Pearson's correlation was significant (p-value <0.05) and strong (r = 0.95), for n = 39 elevation data. Through the simple linear regression we identified that there is a cause-and-effect relationship between the elevation obtained by DTM and the real elevation, obtained in the field, considering that about 95 % (coefficient of determination) of the variability of the elevation obtained by DTM is explained by the elevation obtained with DGPS or vice versa (Fig. 6). The standard error of the mean indicated that the observed elevation values vary by approximately 0.2 m more or less around the estimated mean line.

3.2. Selection of height metrics derived from point clouds generated by SfM for the AGB model fit

From the set of height metrics that were evaluated, we excluded all those considered multicollinear, i.e., with significant correlation (r) (p-value <0.05) and greater than 0.7, as well as those with VIF greater than 5. The remaining 14 metrics were correlated with AGB (Fig. 7), and a high Pearson correlation (r > 0.7) was found to exist between AGB and height metrics derived from point clouds generated by SfM.

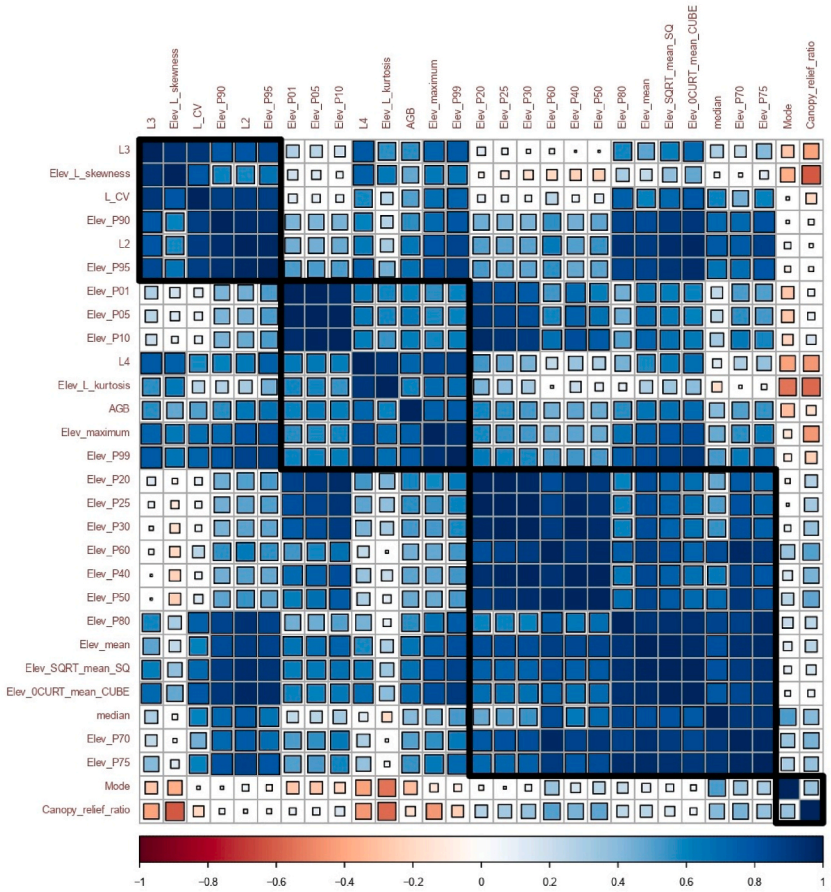

Fig. 7. Graphical representation of Pearson's correlation between the height metrics derived from point clouds generated by SfM and the AGB. Blue color represents positive correlations and red negative correlations. The intensity of the color indicates the strength of the correlation, the more intense the color of the square the higher the correlation.

3.3. Model fit of aboveground dry biomass as a function of height metrics

The observed AGB values of the 39 sampled plots showed normal distribution by the Shapiro-Wilk test (W = 0.9 and p-value = 0.1).

The Stepwise procedure indicated the combination of height metrics with lower AIC value, and was removing from the complete model, step by step, the height metrics (predictor variables) that were not significant (p-value >0.05), until obtaining the best fit for estimating AGB as a function of height metrics derived from point clouds generated by SfM. Therefore, the best fit was obtained as a function of *Elev.MAD.mode* and *Elev.P99* metrics, considered the most significant and best predictors among the height metrics evaluated. The fitted model was given by:

$$\widehat{AGB} = -2,73 - 0,54\ .\ Elev_{MAD\ MODE} + 2,56\ .\ Elev_{P99}$$
$$\left(R^2aj = 0.66;\ RMSE = 0.4122\ Mg\ 0,1\ ha^{-1};\ RMSE = 18.73\%;\ AIC = 45.35\right) \quad (5)$$

where $\widehat{AGB}$ is the estimated aboveground dry woody biomass per 0.1 ha plot (Mg 0,1 ha^{-1}); $Elev_{MAD\ MODE}$ is the mode metric of the absolute overall elevation deviations and $Elev_{P99}$ is the lift metric at the ^{99}th percentile.

The accuracy statistics of the adjusted model were considered satisfactory for the analyzed conditions, considering that remote sensing procedures by remotely piloted aircraft also include variable degrees of inaccuracy that may be related to factors such as the sensor used, the illumination of the environment and the interpretation of the image.

The graphical distribution of the residuals (Fig. 8) and the RMSE value allow the magnitude of the errors resulting from the fitted model to be assessed. The error generated by the fitted equation is approximately 0.41 Mg ha^{-1} or 18.73 % and the residuals were approximately homogeneously distributed (Fig. 8a). Fig. 8b shows that the adjusted model explains 66 % of the total variation in the data at the 1 % significance level, thus demonstrating a good degree of accuracy of the AGB variable as a function of the *Elev.MAD.mode* and *Elev.P99* metrics. The distribution of observed AGB values relative to estimated values (Fig. 8b), as well as the frequency distribution of residual values by residue class (Fig. 8c), show that the highest frequency of these values occurs near zero.

3.4. Validation of the AGB model fitted from the RPA data

Based on the validation results, we found that the prediction error in estimating AGB obtained by the LOOCV cross-validation method was equal to 4.198 Mg ha^{-1}, which corresponds to an average relative error of 19.07 %. This error is considered quite satisfactory since the adjusted model comes from an indirect method of obtaining AGB data. In addition, we must consider the type of vegetation analyzed, with a heterogeneous individual's spatial distribution. The validation obtained an R^2 value equal to 0.61, which is similar to that obtained by the model fit ($R^2 = 0.66$).

3.5. Estimation of aboveground dry biomass stocks for the experimental area

On average, we recorded in the sample area 2205.50 ind ha^{-1} in 2021. The highest density (2383.33 ind ha^{-1}) was observed in the plots subjected to treatment 3 (thinning of 100 % of the basal area of woody individuals with Db ≥ 5 cm, belonging to species with energy potential: *Tachigali vulgaris, Dalbergia miscolobium* and *Pterodon pubescens*) and the lowest (2060 ind ha^{-1}) in the plots subjected to treatment 1 (clear cutting of woody individuals with Db ≥ 5 cm, regardless of species). However, when submitting the data to analysis of variance, considering a randomized block design, we did not detect any significant difference between the densities of

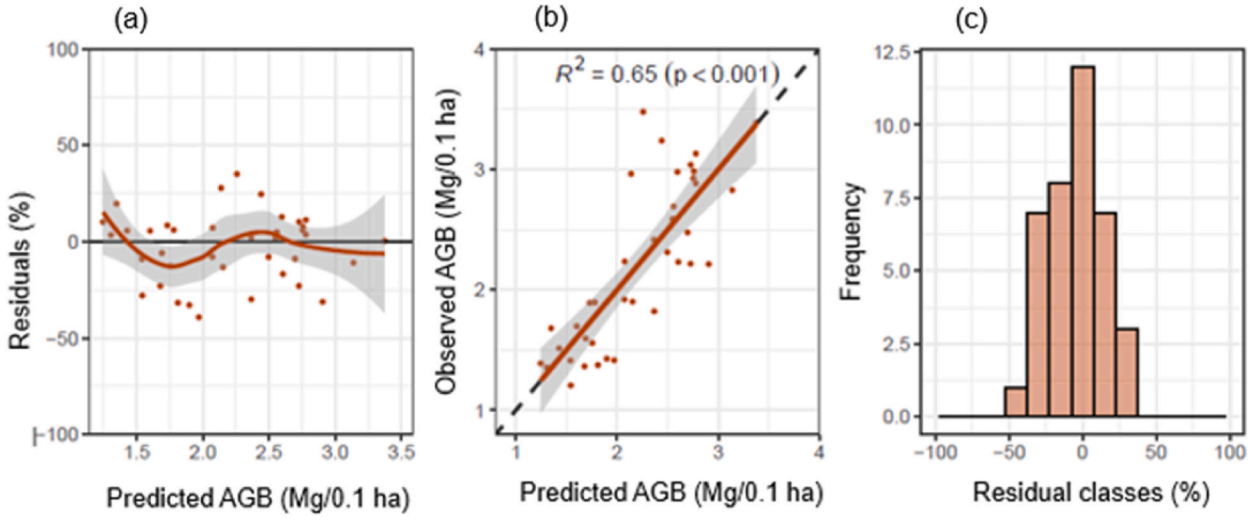

Fig. 8. a) Residues (Mg 0.1 ha^{-1}) as a function of AGB estimated from height metrics derived from SfM-generated point clouds (Mg 0.1 ha^{-1}); b) observed AGB (Mg 0.1 ha^{-1}) versus AGB estimated from those metrics (Mg 0.1 ha^{-1}); and c) frequency distribution of residues by residue class.

individuals recorded in the seven treatments analyzed ($p > 0.05$), indicating that the period of 15 years was sufficient for the vegetation of cerrado *sensu stricto* in thinned areas to recover the density of individuals recorded before logging.

We found that treatments 2 (thinning of 50 % of the basal area of woody individuals with Db $\geq$ 5 cm, regardless of species), 3 (thinning of 100 % of the basal area of woody individuals with Db $\geq$ 5 cm, belonging to species with energy potential: *Dalbergia miscolobium, Pterodon pubescens* and *Tachigali vulgaris*) and 4 (thinning of 50 % of the basal area of woody individuals with Db $\geq$ 5 cm, belonging to species with energy potential: *Dalbergia miscolobium, Pterodon pubescens* and *Tachigali vulgaris*) exceeded the average density recorded in 2021 in the control areas, T6 and T7 (2. 141.67 ind ha^{-1}), with values equal to, respectively, 2316.67 ind ha-1, 2383.33 ind ha^{-1} and 2266.67 ind ha^{-1}.

The observed and estimated AGB values for the areas submitted to the 7 silvicultural treatments showed similar behavior to the density of individuals, with statistically equal mean values, 15 years after the different thinning intensities applied in the areas ($p > 0.05$). However, it is important to note that some treatments that involved thinning of the woody vegetation showed higher stocks of AGB than the control areas (T6 and T7), whose means were 26.65 Mg ha^{-1} for the observed biomass and 26.28 Mg ha-1 for the biomass estimated from the RPA data. This is the case for treatments 3 (thinning of 100 % of the basal area of the woody individuals with Db $\geq$ 5 cm, belonging to the species with energy potential: *Dalbergia miscolobium, Pterodon pubescens* and *Tachigali vulgaris*) and 5 (thinning of 100 % of the basal area of the woody individuals with Db $\geq$ 5 cm, belonging to Tachigali vulgaris). For the observed AGB obtained from the allometric model, the stocks were equal to 29.53 Mg ha^{-1} and 29.80 Mg ha^{-1}, respectively, and for the AGB estimated from RPA data, the stocks were equal to 31.07 Mg ha^{-1} and 27.15 Mg ha^{-1}, respectively.

When comparing the observed and estimated AGB stocks for the 7 treatments, using the analysis of variance, we also found that these stocks are statistically equal, i.e., the average stocks of AGB, observed and estimated, in areas of cerrado *sensu stricto* submitted to the 7 silvicultural treatments are statistically equal ($p > 0.05$).

3.6. Map of aboveground dry biomass estimated from remotely piloted aircraft data

A biomass map with AGB estimates was produced for the entire RPA overflight area (10.4 ha), considering a resolution of 30 m $\times$ 30 m (Fig. 9). We estimated for the total area 255.8 ($\pm$) 2.7 Mg de AGB or 24.6 Mg ha^{-1}. The values of AGB per 30 m $\times$ 30 m subunit ranged from 10.5 to 24.7 Mg.

4. Discussion

4.1. SfM method in digital terrain model building

The SfM method is one of the new approaches to analyzing structures and estimating forest parameters from aerial imagery obtained by an RGB camera aboard RPA. The success of these analyses depends on the ability of the used sensor to capture ground data, i.e., the accuracy and precision of the final AGB estimates are dependent on the quality of the DTM (Kachamba et al., 2016).

Although RGB cameras presents limitations when applied to closed canopy forests, due to the difficulty of passive sensors to

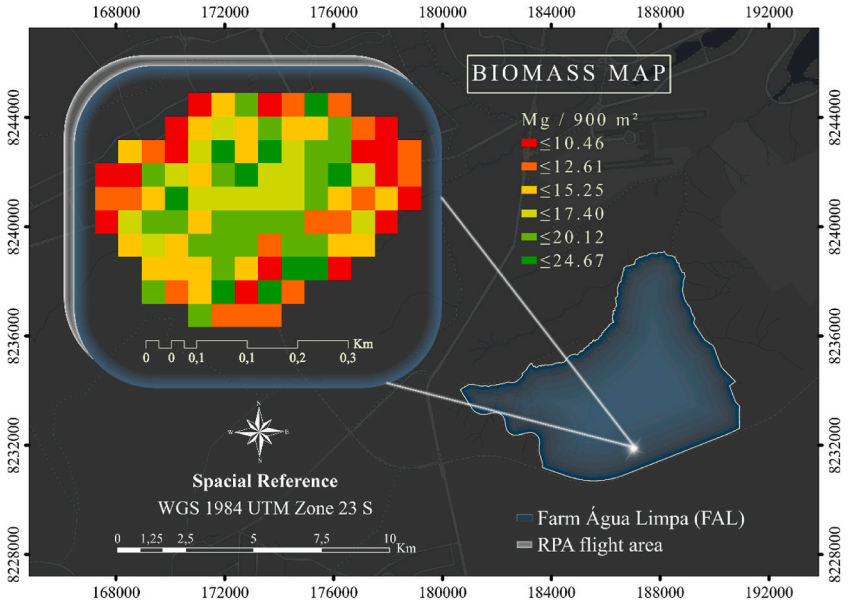

Fig. 9. Estimated dry biomass distribution map (raster) for the RPA flight area (10.4 ha) at 30 m spatial resolution, generated from the AGB equation fitted with height metrics derived from SfM-generated point clouds.

penetrate the canopy, it can be considered a remote sensing technology capable of capturing structural information on forests with relatively sparse canopy, such as the cerrado *sensu stricto*.

Even though the sampling model was specifically calibrated for cerrado *sensu stricto*, the results confirm that structural metrics extracted from photogrammetric point clouds — generated via Structure from Motion (SfM) applied to RPA imagery — are effective in estimating aboveground dry biomass in savanna environments with sparse canopy cover. Similar results have been reported in tropical savannas, such as in Australia, where SfM-derived models provided sufficient topographic accuracy for biomass assessments (Smith et al., 2023). These findings highlight the potential of RPA-based structural data as a high-resolution and cost-effective alternative for biomass monitoring in open-canopy savanna systems. Considering that more than half of the world's forested areas have less than 50 % canopy cover (Hansen et al., 2013), including savannas, SfM has great use potential (DANDOIS and ELLIS, 2010; Mlambo et al., 2017). If the captured images contain the exact geographical position and orientation of the spectral sensor, SfM processing provides high geometric fidelity (Aasen et al., 2018). In this study, because it was a small area (10.4 ha), the 5 GCPs collected were sufficient.

The overlap of the images and the ground sampling distance (GSD) affect the quality of the 2D image reconstruction in 3D (Frey et al., 2018). For the best reconstruction results, it is recommended that the image overlap, and spatial resolution be high (Pix4D Mapper 3.3 User Manual, 2017). Other studies used frontal and lateral overlap between 60 and 85 % in a Brazilian savanna area (Cerrado) and ensured sufficient point matching in post-processing (Batistoti et al., 2019; Kolarik et al., 2020).

To obtain better biomass estimates, Mlambo et al. (2017) compared the laser scanning (LiDAR) method with the SfM method to obtain 3D structural information of a small forest plot (2.3 ha) with a sparse canopy structure in the UK. The authors found SfM to be a suitable and low-cost alternative for forest surveys in open canopy areas in developing countries.

4.2. Metrics derived from point clouds generated by SfM

We selected the best metrics derived from point clouds generated by SfM data to fit a model that accurately estimated aboveground biomass (AGB) in the cerrado *sensu stricto* and enabled the generation of AGB maps for the entire imaged area.

Our biomass estimation approach identified the mode of the median absolute deviation of elevation (*Elev.MAD.mode)* and the 99th percentile of elevation (*Elev.P99)* as the most relevant predictors These metrics are related to canopy height variability and extreme canopy height values, respectively, and align with previous studies focused on estimating aboveground dry volume and biomass (Hernández-Stefanoni et al., 2014; Hirigoyen et al., 2020). Also, in a previous study in a Brazilian savanna (Cerrado) using LiDAR data selected the 98th percentile of canopy height (H98TH) and canopy cover (COV) as key variables for biomass modeling (Costa et al., 2021). Similarly, research in Australian savanna highlighted the quadratic mean canopy height (CHM) as the most explanatory variable, using a conventional RGB camera mounted on a low-cost RPA (Goldbergs et al., 2018).

Overall, these results confirm that structural height metrics derived from point clouds generated by RPAs using Structure from Motion (SfM) represent a viable and promising alternative for estimating biomass in savanna ecosystems. For instance, SfM-based models using RPA imagery have been effectively applied to accurately quantify herbaceous biomass in African savanna areas, with a relative error of approximately 25 % (Taugourdeau et al., 2022). Additionally, this approach has been successfully implemented in Kenyan savannas, providing precise three-dimensional reconstructions of vegetation structure (Shukla et al., 2024). This methodology is particularly well-suited for adaptive monitoring and carbon assessment in selectively managed areas, offering a high-resolution and cost-effective alternative to conventional methods.

4.3. Modeling and estimation of dry biomass with remotely piloted aircraft data

Considered the second largest source of carbon emissions in Brazil, the Cerrado accounted for approximately 17 % of the national emissions in 2023, showing a significant increase compared to previous years (OBSERVATÓRIO DO CLIMA, 2024). Thus, studies that accurately quantify biomass are critical to assessing the storage capacity and carbon emission potential of forests in the atmosphere (Roquette, 2018). Appropriate vegetation carbon management, conservation and restoration models depend on the reliability of this information (Bispo et al., 2020).

Studies conducted in an area of cerrado *sensu stricto* at Fazenda Água Limpa - FAL, quantified AGB using direct measurements (cutting and weighing). Vale et al. (2005) recorded an average production of 12.4 Mg ha^{-1} for and Rezende et al. (2006) recorded 9.9 $\pm$ 1.1 Mg ha^{-1} for AGB and 4.9 $\pm$ 0.5 Mg ha^{-1} for C. The AGB values obtained in this study exceeded those reported by these authors by approximately 50 % and 60 %, respectively, likely due to differences in management practices, species diversity, and structural variability of the area.

We emphasize that the unequal variations observed in the quantification of biomass in the present study in relation to those previously mentioned are certainly related to factors such as the influence of the applied silvicultural treatments on the growth of the woody community over time, the great diversity of species, the high variability of stem and canopy shape, the conservation status of the area, the protection of the area from forest fires, and climate variations.

Aiming to optimize the time and cost spent on estimates obtained by direct methods, statistical models that integrate remote sensing measurements and field plots have been successfully applied both in the Amazon (Espindola et al., 2012; Chen et al., 2015; d; Oliveira et al., 2021), and in the Cerrado (Ribeiro et al., 2011; Bispo et al., 2020; Costa et al., 2021).

Using only LiDAR data to map the total biomass of an area encompassing the three Cerrado physiognomic forms (forest, savanna and campo), in the states of Goiás and Minas Gerais, Costa et al. (2021) fitted a general model with an R^2 aj of 0.8 and an RMSE% of 33.4 %. The authors evaluated the estimation error for each formation separately and thus obtained an RMSE% of 43.96 % for the

savanna area. The model developed in this study showed higher precision (RMSE% = 14 %), possibly due to the relatively small study area with little structural variation. Although the analyzed area is limited, understanding the broader biome context in wich it is located is essential to assess the model's potential applicability. As stated in the introduction, the Brazilian Cerrado encompasses more than 2 million km^2 of the national territory (Lahsen et al., 2016). Within this vast biome, the cerrado *sensu stricto* represents one of the main vegetation types, and the model developed here demonstrates potential applicability to areas with similar structural characteristics. Regarding the mean biomass estimate, Costa et al. (2021) found 41 Mg ha^{-1} for AGB, surpassing the estimate found in this study (25 Mg ha^{-1}) by about 40 %, which can be explained by the fact that non-woody vegetation was included in the estimate.

Although we acknowledge that including other physiognomies and environmental variables could enhance model robustness, this study provides a proof of concept with practical and scalable applicability to cerrado *sensu stricto* areas under similar environmental conditions. Furthermore, the results indicate potential for generating continuous biomass maps, contributing to methodological advances and supporting public policies focused on Cerrado conservation and monitoring.

Other authors have produced more accurate and reliable models when combining LiDAR data and RGB photogrammetry in natural forests (Otero et al., 2018; Mcclelland; Van Aardt; Hale, 2019; d; Oliveira et al., 2021). By combining the use of field plots, LiDAR data and satellite imagery (Landsat8 and ALOS-2/Palsar-2), Bispo et al. (2020) found R^2 aj = 0.9 and RMSE% = 13 %. They subsequently produced a high resolution (30 m) biomass map to predict the total biomass present in a region of the Rio Vermelho watershed - GO (area covered by LiDAR flight: 1,082,460 ha). They obtained an average of 18.66 Mg ha^{-1}, ranging from 0 to 90 Mg ha^{-1} per pixel. These results are not comparable to those found for the AGB map in this study due to the different sensors used (LiDAR x RPA) and the discrepant area sizes (1,082,460 ha × 10.4 ha).

The use of LiDAR technology is limited due to its high data acquisition costs. However, with relatively low costs, remotely piloted aircraft (RPAs) have been increasingly used in small forests and forests with canopy cover below 50 % (Kachamba et al., 2016; Tang; Shao, 2015). For the Cerrado, we found studies that used RGB imagery aboard RPAs aimed at detecting invasive plants (Nascente et al., 2022), using vegetation indices for monitoring (González-Jaramillo et al., 2019), or estimating the fuel material of the biome (Souza et al., 2018).

In the present study, even with the use of a passive sensor, it was possible to develop a highly accurate biomass model, owing to the structural characteristics of the Cerrado, which facilitate the construction of a precise digital terrain model (DTM). This underscores the potential of photogrammetric approaches under such conditions. Conversely, in dense forest environments, photogrammetry alone is unlikely to yield an accurate DTM; in such cases, prior LiDAR coverage would be required to ensure model reliability, as demonstrated by D'OLIVEIRA et al. (2021).

5. Conclusions

Our study confirmed the effectiveness of SfM photogrammetry using RGB imagery acquired by RPA in estimating AGB in cerrado *sensu stricto* formations. The statistical model developed, based on the *Elev.MAD.mode* and *Elev.P99* height metrics, showed satisfactory accuracy and enabled the generation of high-resolution AGB maps for the entire imaged area.

Although limited in spatial extent, the results are consistent with previous studies and highlight the potential of RGB-based SfM methods as a low-cost and effective alternative for biomass monitoring in open-canopy savanna ecosystems. Notably, the study area underwent selective logging treatments, and yet, 15 years later, biomass stocks estimated via RPA were statistically similar to those of control areas, indicating regrowth and recovery potential.

The study also reinforces the relevance of accurate AGB mapping to support carbon monitoring initiatives and assess land degradation, especially in a biome under increasing anthropogenic pressure such as the Cerrado.

Challenges remain, including the need to improve model generalization to more heterogeneous physiognomies and incorporate multi-date imagery for temporal monitoring. Future research should explore hybrid approaches combining RGB SfM data with other sensors (e.g., multispectral or LiDAR), as well as the use of machine learning techniques to refine biomass estimation and expand applicability to broader landscapes.

Furthermore, the model's applicability is constrained by the structural characteristics of the Cerrado; it was developed and validated specifically for homogeneous cerrado *sensu stricto* areas. While these conditions allowed the generation of accurate digital terrain models (DTMs) and high-precision biomass estimates, the approach may not be directly transferable to denser or more heterogeneous forested environments. In such cases, prior LiDAR coverage would likely be required to ensure reliable DTM construction and maintain the accuracy and reproducibility of biomass estimates. This contextualization emphasizes both the strengths and the limitations of RGB-based SfM photogrammetry for biomass monitoring and provides guidance for its adaptation to other biomes and broader landscapes.

CRediT authorship contribution statement

Paola Aires Lócio de Alencar: Writing – original draft, Validation, Software, Methodology, Investigation, Formal analysis, Conceptualization. **Alba Valéria Rezende:** Writing – review & editing, Conceptualization. **Marcus Vinicio Neves d'Oliveira:** Writing – review & editing, Validation, Supervision, Software, Methodology, Data curation, Conceptualization. **Eder Pereira Miguel:** Validation, Methodology, Data curation. **Hallefy Junio de Souza:** Validation, Software, Methodology, Investigation. **Roberta Franco Pereira de Queiroz:** Validation, Software, Methodology, Investigation.

Ethical Statement

Hereby, I, Paola Aires Lócio de Alencar, consciously assure that for the manuscript "Modeling aboveground dry biomass in Brazilian savanna using Remotely Piloted Aircraft (RPA) data after 15 years of reduced impact selective logging" the following is fulfilled:

1) This material is the authors' own original work, which has not been previously published elsewhere.
2) The paper is not currently being considered for publication elsewhere.
3) The paper reflects the authors' own research and analysis in a truthful and complete manner.
4) The paper properly credits the meaningful contributions of co-authors and co-researchers.
5) The results are appropriately placed in the context of prior and existing research.
6) All sources used are properly disclosed (correct citation).
7) All authors have been personally and actively involved in substantial work leading to the paper, and will take public responsibility for its content.

I agree with the above statements and declare that this submission follows the policies of Solid State Ionics as outlined in the Guide for Authors and in the Ethical Statement.

Declaration of competing interest

The authors declare that they have no known competing financial interests or personal relationships that could have appeared to influence the work reported in this paper.

Acknowledgements

This study was financed in part by the Coordenação de Aperfeiçoamento de Pessoal de Nível Superior – Brasil (CAPES) – Finance Code 001.

Data availability

Data will be made available on request.

References

Aasen, H., Honkavaara, E., Lucieer, A., Zarco-Tejada, P.J., 2018. Quantitative remote sensing at ultra-high resolution with UAV spectroscopy: a review of sensor technology, measurement procedures, and data correction workflows. *Remote sensing*. Remote Sens. 10 (7), 1091.
Abdala, G.C., Caldas, L.S., Haridasan, M., Eiten, G., 1998. Above and belowground organic matter and root: shoot ratio in a cerrado in central Brazil. Brazilian J. Ecol. 2 (1), 11–23.
Akaike, H., 1973. Information theory and an extension of the maximum likelihood principle. In: International Symposium on Information Theory, 2., 1973, Budapest. *Proceedings*. Akademiai Kiado, Budapest, pp. 267–281.
Almeida, D.R.A., Broadbent, E.N., Oliveira, S. N. de, Silva, C.A., Resende, F.M., 2023. UAV-Based canopy height models predict biomass in Brazilian neotropical savannas. Remote Sens. 15 (1), 112.
Alvares, C.A., Stape, J.L., Sentelhas, P.C., Gonçalves, J.D.M., Sparovek, G., 2013. Köppen's climate classification map for Brazil. Meteorol. Z. 22 (6), 711–728.
Araujo, D.M., et al., 2024. RGB drone imagery for estimating biomass in savanna ecosystems: a case study in the cerrado. Remote Sens. Appl.: Soc. Environ. 33, 100941.
Bazzo, A., et al., 2024. Remote sensing-based biomass estimation for carbon market integration in tropical savannas. Rem. Sens. Environ. 312, 114023.
Bera, E.F., Siqueira, P.R., Santos, J. R. dos, Keller, M., 2022. Structure-from-Motion photogrammetry in open-canopy tropical ecosystems: a viable alternative for forest structural mapping. Remote Sens. 14 (3), 550.
Beuchle, R., Grecchi, R.C., Shimabukuro, Y.E., Seliger, R., et al., 2015. Land cover changes in the Brazilian Cerrado and Caatinga biomes from 1990 to 2010. Appl. Geogr. 58, 116–127.
Bispo, P.D.C., Rodríguez-Veiga, P., Zimbres, B., Miranda, C.O., et al., 2020. Woody aboveground biomass mapping of the Brazilian savanna with a multi-sensor and machine learning approach. Remote Sens. 12 (17), 2685.
BRASIL. Ministério do Meio Ambiente, 2011. Plano De Ação Para Prevenção E Controle do Desmatamento E Das Queimadas: Cerrado. MMA, Brasília, p. 200.
Burkholder, B.K., et al., 2021. Savanna fire regimes shape carbon balance and storage in South American ecosystems. Glob. Change Biol. 27, 3924–3940.
Costa, M.B.T., Silva, C.A., Broadbent, E.N., Leite, R.V., et al., 2021. Beyond trees: mapping total aboveground biomass density in the Brazilian savanna using high-density UAV-lidar data. For. Ecol. Manag. 491, 119155.
Cunliffe, A.M., Anderson, K., Brazier, R.E., 2021. UAVs reveal spatial variation in grazing impacts within extensive rangelands. Remote Sens. 13 (4), 693.
Dandois, J.P., Ellis, E.C., 2010. Remote sensing of vegetation structure using computer vision. Remote Sens. 2 (4), 1157–1176.
Díaz-Varela, R.A., et al., 2023. UAV-based estimation of aboveground biomass and carbon stocks in semi-arid African woodlands. For. Ecol. Manag. 543, 121110.
DJI, 2017. Phantom 4 Pro/pro+ User Manual.
D'Oliveira, M.V.N., Figueiredo, E.O., Papa, D. de A., 2014. Uso Do LIDAR Como Ferramenta Para O Manejo De Precisão Em Florestas Tropicais. Embrapa, Acre.
D'Oliveira, M.V.N., et al., 2021. Impacts of selective logging on Amazon forest canopy structure and biomass with a LiDAR and photogrammetric survey sequence. For. Ecol. Manag. 500, 119648.
Duvert, C., et al., 2020. Net landscape carbon balance of a tropical savanna: fire and aquatic export. Glob. Change Biol. 26 (10), 5899–5913.
Frey, J., et al., 2018. UAV photogrammetry of forests as a vulnerable process. A sensitivity analysis for SfM RGB-image pipeline. Remote Sens. 10 (6), 912.
González-Jaramillo, V., Fries, A., Bendix, J., 2019. Monitoring the forest recovery after fire disturbance using UAVs and vegetation indices. Remote Sens. 11 (7), 770.
Gülci, S., Akay, A.E., Yilmaz, O., 2023. Applications of UAV-based biomass estimation for forest carbon monitoring and REDD+ strategies. For. Pol. Econ. 150, 102999.
Hansen, M.C., et al., 2013. High-resolution global maps of 21st-century forest cover change. Science 342 (6160), 850–853.
Hernández-Stefanoni, J.L., et al., 2014. Combining field data and lidar to estimate above-ground biomass in tropical dry forests. For. Ecol. Manag. 312, 28–40.

Hirigoyen, A., et al., 2020. Comparison of structure-from-motion photogrammetry and LiDAR for estimating forest biomass in tropical dry forests. For. Ecol. Manag. 475, 118369.
Kachamba, D.J., et al., 2016. Biomass estimation using photogrammetric data from UAV imagery in open forests. Remote Sens. 8 (11), 968.
Koh, L.P., Wich, S.A., 2012. Dawn of drone ecology: low-cost autonomous aerial vehicles for conservation. Trop. Conserv. Sci. 5 (2), 121–132.
Kuhn, M., 2008. Building predictive models in R using the caret package. J. Stat. Software 28 (5), 1–26.
Lahsen, M., et al., 2016. The politics of environmental data: observational satellites and the Brazilian Amazon. Soc. Stud. Sci. 46 (1), 3–24.
Mayr, M.I., Assmann, T., Heurich, M., 2023. UAV-based structure-from-motion point clouds improve biomass modeling in temperate open forests. For. Ecol. Manag. 532, 120178.
Mlambo, R., Woodhouse, I.H., Mutanga, O., 2017. Structure from motion (SfM) photogrammetry: a low-cost, effective tool for savanna rangeland monitoring. Int. J. Rem. Sens. 38 (21), 5988–6005.
OBSERVATÓRIO DO CLIMA, 2024. Análise das emissões brasileiras de GEE – SEEG 2024. Disponível em: https://seeg.eco.br/.
Puliti, S., et al., 2021. Estimation of forest growing stock volume with UAV laser scanning data: can it be done without field data? Remote Sens. 13 (6), 1094.
Pugh, T.A.M., et al., 2019. Role of the land biosphere in contemporary climate change. Nat. Clim. Change 9, 699–706.
Rezende, A.V., Figueiredo, E.O., Davide, A.C., 2006. Biomassa E Carbono em Sistemas De Uso Da Terra No Cerrado, 122. Embrapa Cerrados, Documentos.
Roitman, I., et al., 2018. Mapping forest biomass with remote sensing: an approach to inform REDD+ strategies in the tropics. Carbon Bal. Manag. 13 (1).
Rügner, H., et al., 2022. Assessing long-term savanna fire regimes and carbon dynamics using remote sensing. Sci. Total Environ. 806, 150843.
Sanky, T.T., et al., 2022. Monitoring vegetation structural changes in savannas using UAV-SfM metrics. Remote Sens. 14 (2), 403.
Shin, Y., Lee, H., Lee, D., 2018. Estimating forest biomass using UAV-based photogrammetric point clouds. Remote Sens. 10 (12), 1839.
Shukla, P.R., et al., 2019. IPCC special report on climate change and land. IPCC.
Shukla, R., et al., 2024. UAV-based biomass estimation in Kenyan savannas: assessing variability and accuracy. Ecol. Indic. 158, 111664.
Silva, J.C., Matos, I.S., Santos, R.A., 2023. UAV-derived metrics for biomass mapping in savanna-like ecosystems: a small-scale validation. J. Environ. Manag. 336, 117642.
Smith, J., et al., 2023. Assessment of UAV-based Structure from motion photogrammetry for biomass estimation in tropical savanna landscapes. Geomorphology 457, 108262.
Taugourdeau, S., et al., 2022. Estimating herbaceous aboveground biomass in Sahelian rangelands using SfM data. Ecol. Evol. 12 (5), e8867.
Vale, A. T. do, Ferraz, S.F.B., Rezende, A.V., 2005. Estimativas de biomassa e carbono em área de cerrado sensu stricto. Rev. Arvore 29 (1), 111–118.
Walston, L.J., et al., 2023. Aboveground biomass estimation using UAVs: a global synthesis of accuracy and scale. Ecol. Indic. 147, 109891.
Wulder, M.A., et al., 2021. New perspectives on remote sensing of forest inventory and change. Rem. Sens. Environ. 255, 112276.
Zar, J.H., 1999. Biostatistical Analysis, fourth ed. Prentice Hall, New Jersey.